



Synthesis and properties of highly organosoluble aromatic polyimides containing *N*-(4-(di(1*H*-indole-3-yl)methyl)phenyl) moieties

High Performance Polymers
2020, Vol. 32(1) 83–90
© The Author(s) 2019
Article reuse guidelines:
sagepub.com/journals-permissions
DOI: 10.1177/0954008319853031
journals.sagepub.com/home/hip



Sedigheh Khalili and Zahra Rafiee¹

Abstract

A new diamine monomer containing indole unit, 3,5-diamino-*N*-(4-(di(1*H*-indol-3-yl)methyl)phenyl)benzamide, was successfully synthesized and applied in the preparation of a series of polyimides (PIs) via a conventional two-step polymerization procedure with three aromatic tetracarboxylic dianhydrides. The prepared polymers showed excellent solubility in organic solvents such as *N*-methyl-2-pyrrolidinone (NMP), *N,N*-dimethylacetamide, and *N,N*-dimethylformamide. Flexible and strong films of PIs were obtained via casting from their solutions. The glass transition temperature of these polymers was in the range of 223–264°C. They were fairly stable up to a temperature around 300°C and lost 10% weight at 372°C in nitrogen atmosphere. All of the polymers revealed absorption maxima around 323 nm with a fluorescence emission maxima around 378–406 nm in NMP. The cyclic voltammetry of the PIs exhibited an oxidation wave with a peak at 1.07 V. The resulting polymer films had tensile strengths from 83 MPa to 107 MPa, elongates at break of 7–10%, and tensile moduli of 2.2–2.3 GPa.

Keywords

Polyimide, *N*-(4-(di(1*H*-indol-3-yl)methyl)phenyl)-containing diamine, direct polycondensation

Introduction

Indole or 1*H*-benzo[*b*]pyrrole, the heteroaromatic structure alike carbazole, is ever-present in biological and biochemical heterocyclic structure and due to its exceptional chemical, electrical, and optical properties has attracted considerable attention in the fabrication of pharmaceuticals including anticancer,¹ anti-rheumatoid,² antioxidant,³ anti-HIV,⁴ antiproliferative,⁵ anti-tubulin,⁶ antituberculosis,⁷ antibacterial,⁸ and anti-inflammatory.⁹ The polymers based on indole have been used for the applications in electronics, electrocatalysis, anode materials, anticorrosion coatings, and biological areas.^{10–13} Additionally, the indole group was considered as a valid substitute of the carbazole moiety. Polymers containing carbazole groups have been extensively studied and employed in photoconductivity and photorefractive materials owing to its excellent photoconductivity properties.^{14,15} Nevertheless, in spite of the good results, carbazole-based materials suffer from some drawbacks that can limit their technical applications. These drawbacks concern the very high glass transition temperature of the related polymers, the poor availability, and the carbazole high molecular symmetry. Unfortunately, only very few carbazole derivatives are available and they are

often expensive and difficult to synthesize or modify. The poor availability of the carbazole group to be modified in its electronic and morphological characteristics constitutes a factor limiting the potential tunability of materials. Indeed, many and interesting indole derivatives can be purchased on the chemical market. The electronic nature of the different available substituents on the indole ring can determine the electron donor behavior that is typical of the indolyl moiety.

Aromatic polyimides (PIs) are recognized as a significant class of high-performance polymers owing to their excellent thermal and thermo-oxidative stability, high mechanical strength, chemicals resistance, low dielectric constant, and refractive index.^{16,17} Hence, these macromolecules have been applied in diverse applications such as

Department of Chemistry, Yasouj University, Yasouj, Islamic Republic of Iran

Corresponding author:

Zahra Rafiee, Department of Chemistry, Yasouj University, Yasouj 75918-74831, Islamic Republic of Iran.
Emails: z.rafaee@mail.yu.ac.ir; zahrarafee2004@yahoo.com

microelectronics, aerospace, automotive, optoelectronics, liquid crystal display, composite matrices, gas separation membranes, adhesives, coatings, and foams.^{18–31} The chief drawback of aromatic PIs is their infusibility and low solubility in common organic solvents which make them difficult to process, thus restraining their applications. Many structural modifications have been applied to overcome these limitations.^{32–38} The properties of the PIs are largely dependent on their chemical structure. Hence, significant attention has been given to synthesis of novel diamine and dianhydride monomers possessing exceptional features.

In this article, a new *N*-(4-(di(1*H*-indole-3-yl)methyl)-phenyl)-containing heteroaromatic diamine has been synthesized and aromatic PIs have been prepared by the reaction of this diamine monomer with three commercially available tetracarboxylic dianhydrides. Since the novel indole-based polymers possess indole rings in the polymer chain, they are expected to be endowed with good thermal stability, exceptional photoluminescence, and good electroactivity, which would warrant their potential of applications for advanced high-performance materials such as optoelectronics, automotive, aircraft, and spacecraft industry.

Experimental section

Materials

All chemicals were purchased from Merck Chemical Co (Darmstadt, Germany) and Aldrich Chemical Co. (Milwaukee, Wisconsin, USA). Indole, 4-nitrobenzaldehyde, ammonium acetate, hydrazine monohydrate, 10% palladium on activated carbon (Pd/C), and 3,5-dinitrobenzoyl chloride were purchased from Merck and were used as received. 3,3',4,4'-Benzophenonetetracarboxylic dianhydride (BTDA; from Merck) and 4,4'-(hexafluoroisopropylidene)diphthalic anhydride (6FDA; from Aldrich) were recrystallized from acetic anhydride before use. Pyromellitic dianhydride (PMDA; from Merck) was purified by sublimation. *N*-methyl-2-pyrrolidinone (NMP) and *N,N*-dimethylacetamide (DMAc) were purified by distillation under reduced pressure over barium oxide.

Techniques

Proton nuclear and carbon-13 magnetic resonance (¹H NMR and ¹³C NMR) spectra were recorded on Bruker Avance 400 MHz spectrometer in dimethyl sulfoxide-*d*₆ (DMSO-*d*₆). Inherent viscosities were measured by a standard procedure using a Cannon-Fenske routine viscometer (Germany) at the concentration of 0.5 g dL⁻¹ at 25°C. The number average molecular weight (*M*_n) and weight average molecular weight (*M*_w) values were determined by gel permeation chromatography. Fourier transform infrared spectroscopy (FTIR) spectra were recorded with a Jasco-680 spectrometer (Japan) in the range of 400–4000 cm⁻¹.

Vibration bands were reported as wave number (cm⁻¹). FTIR spectra of all samples were collected by making their pellets in potassium bromide (KBr) as a medium. The diffraction pattern of related materials was recorded in the reflection mode using a Bruker, D8 Advance diffractometer. Nickel filtered copper *K*_α radiation (radiation wavelength, λ = 0.154 nm) was produced at an operating voltage of 45 kV and a current of 100 mA. The redox behavior was investigated with cyclic voltammetry (CV) on a potentiostat EG&G Co, PARSTAT 2273, (Oak Ridge, TN, USA) instrument. It was conducted for the dipped polymer film on the working electrode in dry acetonitrile containing tetrabutylammonium hexafluorophosphate (0.1 M) as an electrolyte. Thermogravimetric analysis (TGA) and differential scanning calorimetry (DSC) are performed with a STA503 win TA at a heating rate of 10°C min⁻¹ from 25°C to 800°C under a nitrogen atmosphere.

Monomer synthesis

Synthesis of 3,3'-((4-nitrophenyl)methylene)bis(1*H*-indole) (3). A mixture of indole (1.55 g, 13.23 mmol) and 4-nitrobenzaldehyde (1.00 g, 6.62 mmol) in glacial acetic acid (5 mL) was refluxed for 6 h. The progress of the reaction was monitored by thin layer chromatography (TLC). After cooling, the reaction mixture was poured into 30 mL of H₂O with constant stirring, producing a precipitate that was washed thoroughly with diethyl ether, collected by filtration, and dried at room temperature. Yield: 86%. m.p.: 225–227°C. FTIR (KBr, cm⁻¹): 3427 (N–H stretch), 1507, 1331 (–NO₂ stretch). ¹H NMR (DMSO-*d*₆, ppm): δ: 11.10 (s, 2 H, N–H), 8.21–6.89 (m, 14 H, Ar), 6.05 (s, 1 H); ¹³C NMR; DMSO-*d*₆, ppm): δ: 154.00, 146.63, 146.63, 137.47, 137.47, 130.32, 130.32, 127.24, 124.73, 124.73, 124.28, 124.28, 121.97, 121.97, 119.78, 119.78, 119.29, 119.29, 117.55, 117.55, 112.46, 112.46, 40.35.

Synthesis of 4-(di(1*H*-Indole-3-yl)methyl)aniline (4). Into a 50-mL two-necked flask, 0.200 g (0.544 mmol) of nitro compound 3, 0.01 g of 10% Pd/C, and 10 mL of ethanol were introduced. The suspension solution was refluxed, and 3 mL of hydrazine monohydrate was added dropwise. After the complete addition, the reaction was continued at reflux temperature for another 12 h. To the suspension, 10 mL of tetrahydrofuran (THF) was added to redissolve the precipitated product, and refluxing was continued for 1 h. The reaction mixture was filtered to remove the Pd/C and the filtrate was distilled to remove the solvent. The crude product recrystallized from ethanol and dried at 80°C under vacuum to give 0.143 g (yield: 78%) of compound 4. m.p.: 230–232°C. FTIR (KBr, cm⁻¹): 3413, 3386 and 3320 (N–H stretch). ¹H NMR (DMSO-*d*₆, ppm): δ: 10.69 (s, 2 H, NH), 7.38–6.51 (m, 14 H, Ar–H), 5.65 (s, 1 H, C–H), 4.83 (s, 2 H, NH₂). ¹³C NMR (DMSO-*d*₆, ppm): δ: 144.01, 137.10, 137.01, 129.59, 129.59, 126.97, 126.97, 123.40, 123.40,

120.86, 120.86, 119.75, 119.75, 118.48, 118.48, 118.08, 118.08, 115.51, 115.51, 110.72, 110.72, 39.88.

Synthesis of 4-(di(1H-indole-3-yl)methyl)aniline (4). To a 25 mL round-bottomed flask, 0.20 g (0.593 mmol) of the compound 4 in 5 mL of dry DMAc was added. The reaction mixture was cooled in an ice H₂O bath. To this mixture, 0.137 g (0.593 mmol) of 3,5-dinitrobenzoyl chloride (5) in 2 mL of DMAc was added dropwise. The mixture was stirred in ice bath for 3 h, and then 0.083 mL of triethylamine was added. The mixture was stirred in ice bath for 2 h and at room temperature overnight. The resulting mixture was poured into 25/5 mL of cold water/concentrated hydrochloric acid. The precipitate was collected by filtration and purified by recrystallization from *N,N*-dimethylformamide (DMF)/H₂O to afford dinitro compound 6 in 87% yield; m.p.: 330–332°C. FTIR (KBr, cm⁻¹): 3426, 3264 (N–H stretch), 1650 (C=O stretch), 1546, and 1342 (–NO₂ stretch). ¹H NMR (DMSO-*d*₆, ppm): δ: 10.85 (s, 2 H, N–H indole), 10.53 (s, 1 H, NH–C=O), 9.17–9.16 (d, 2 H, Ar–H), 9.01 (s, 1 H, Ar–H), 6.86–7.72 (Ar–H), 5.85 (s, 1 H, C–H).

Synthesis of 3,5-diamino-*N*-(4-(di(1H-indol-3-yl)methyl)phenyl)benzamide (7). Into a two-necked flask, 0.100 g (0.188 mmol) of the dinitro compound 6, 0.01 g of 10% Pd/C, and 10 mL of ethanol were introduced. The suspension solution was heated to reflux, and 3 mL of hydrazine monohydrate was added dropwise. After the complete addition, the reaction was continued at reflux temperature for another 12 h. To the suspension, 5 mL of THF was added to redissolve the precipitated product, and refluxing was continued for 1 h. The mixture was filtered to remove the Pd/C and the filtrate was distilled to remove the solvent. The yield was 81%; m.p.: 263–265°C. FTIR (KBr, cm⁻¹): 3461, 3436, 3361, 3326 (N–H stretch), 1652 (C=O stretch). ¹H NMR (DMSO-*d*₆, ppm): δ: 10.83 (s, 2 H, N–H indole), 9.89 (s, 1 H, N–H), 8.34–6.00 (Ar–H), 5.80 (s, 1 H), 4.00 (s, 4 H, N–H); ¹³C NMR (DMSO-*d*₆, ppm): 167.92, 144.06, 138.71, 135.79, 130.11, 129.42, 128.62, 127.97, 122.63, 122.14, 118.67, 117.36, 110.56, 110.16, 100.74.

Polymer synthesis

The polymers were prepared via a two-step method; 0.0925 g (0.424 mmol) of PMDA was added gradually into a solution of 0.2000 g (0.424 mmol) of diamine 7 in 3 mL of dehydrated NMP under nitrogen atmosphere with stirring. The mixture was stirred at room temperature for 24 h to produce a viscous poly(amic acid) (PAA) solution. The inherent viscosity of the PAA in DMAc was 0.52 dL g⁻¹, measured at a concentration of 0.50 g dL⁻¹ at 25°C. The PAA was converted into PI by either a thermal or chemical imidization procedure. For the thermal imidization, the PAA film was obtained by casting from the reaction polymer solution onto a glass plate and drying at 90°C overnight

under vacuum. Then, the PAA film was transformed into PI by sequentially heated at 110°C, 150°C, 180°C, 210°C, 230°C, and 280°C for 30 min each. Meanwhile, the chemical imidization was carried out via the addition of 3 mL of an acetic anhydride/pyridine (5:4, v/v) mixture into the PAA solution with stirring at room temperature. Then, the reaction mixture was heated to 100°C for 3 h to yield a homogeneous PI solution. The homogeneous polymer solution was poured slowly into methanol to give a fibrous precipitate, which was collected by filtration, washed thoroughly with methanol, and dried at 100°C under vacuum. The other PIs (PI-b and PI-c) were prepared using a similar procedure.

PAA: FTIR (KBr, cm⁻¹): ν = 3500–2700 (br), 1776 (m), 1743 (s), 1654 (s), 1608 (s), 1502 (s), 1463 (m), 1446 (m), 1294 (m), 1088 (m), 987 (m), 845 (m), 793 (m), 758 (m), 672 (m).

PI-a-II: M_n = 14600, M_w = 21800. FTIR (KBr, cm⁻¹): ν = 3379 (N–H stretch), 3036 (=C–H stretch), 1778 (asymmetrical C=O, imide), 1725 (symmetrical C=O, imide), 1658 (C=O stretch, amide), 1367 (C–N stretch), 725 (imide ring deformation). ¹H NMR (DMSO-*d*₆, ppm): δ: 10.86 (s, 2 H, N–H indole), 9.93 (s, 1 H, N–H), 8.54–7.00 (m, 19 H, Ar–H), 5.75 (s, 1 H). Anal. calcd. for (C₄₀H₂₃N₅O₅)_n: C, 73.50; H, 3.55; N, 10.71; Found: C, 73.88; H, 3.73; N, 10.68.

PI-b-II: M_n = 16400, M_w = 23900. ¹H NMR (DMSO-*d*₆, ppm): δ: 10.92 (s, 2 H, N–H indole), 9.86 (s, 1 H, N–H), 8.76–6.98 (m, 23 H, Ar–H), 5.49 (s, 1 H). Anal. calcd. for (C₄₇H₂₇N₅O₆)_n: C, 74.50; H, 3.59; N, 9.24; Found: C, 74.73; H, 3.69; N, 9.44.

PI-c-II: M_n = 15500, M_w = 21800. ¹H NMR (DMSO-*d*₆, ppm): δ: 10.98 (s, 2 H, N–H indole), 10.01 (s, 1 H, N–H), 8.77–7.06 (m, 23 H, Ar–H), 5.66 (s, 1 H). Anal. calcd. for (C₄₉H₂₇F₆N₅O₅)_n: C, 66.90; H, 3.09; N, 7.96; Found: C, 67.01; H, 3.11; N, 8.02.

Results and discussion

Monomer synthesis

The aromatic diamine, 3,5-diamino-*N*-(4-(di(1H-indol-3-yl)methyl)phenyl)benzamide (7), was synthesized through four-step synthetic route according to Figure 1. 3,3'-(4-Nitrophenyl)methylene)bis(1H-indole) (3) was prepared by electrophilic substitution reaction of indole and 4-nitrobenzaldehyde in the presence of acetic acid as the activating agent. The catalytic hydrogenation of the nitro compound 3 to 4-(di(1H-indole-3-yl)methyl)aniline (4) was accomplished using hydrazine monohydrate and a catalytic amount of Pd/C. The dinitro compound 6 was synthesized by the amination reaction of compound 4 with 3,5-dinitrobenzoyl chloride (5), followed by hydrazine Pd/C-catalytic reduction. The purity of the intermediate compounds 3, 4, and 6 and the diamine monomer 7 was checked by TLC, which showed one spot in an ethylacetate/cyclohexane mixture (50:50). The chemical structures of the intermediate compounds 3, 4, and 6 and the diamine

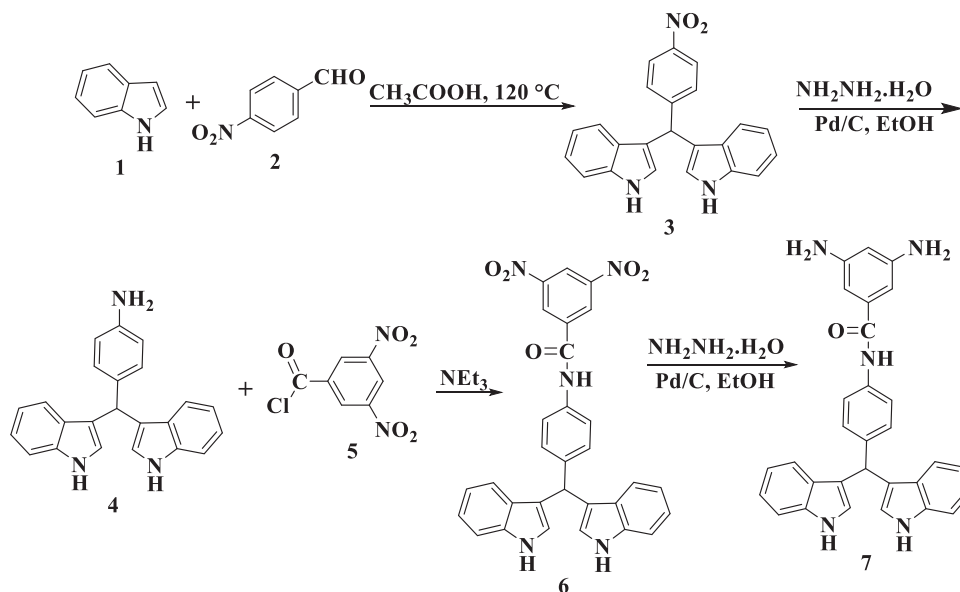


Figure 1. Synthesis of diamine 7.

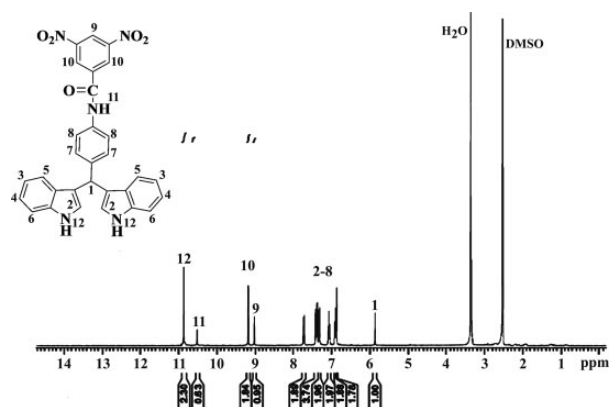


Figure 2. ^1H NMR spectrum of dinitro 6 in $\text{DMSO}-d_6$ solution. ^1H NMR: Proton nuclear magnetic resonance; $\text{DMSO}-d_6$: dimethyl sulfoxide- d_6 .

monomer 7 were proven by FTIR, ^1H NMR and ^{13}C NMR spectroscopic techniques. The transformation of nitro to amino functionality could be monitored by the change of FTIR spectra. The nitro groups of compounds 3 and 6 gave two characteristic bands around 1546 and 1342 cm^{-1} ($-\text{NO}_2$ asymmetric and symmetric stretching), respectively. After reduction, the characteristic absorptions of the nitro group disappeared and the amino group showed the typical N–H stretching absorption pair in the region of 3461 – 3326 cm^{-1} . The ^1H NMR spectra of the compounds 6 and 7 are shown in Figures 2 and 3. These spectra agree with the proposed molecular structure of these compounds. Besides, the peak positions in the ^{13}C NMR spectrum of the diamine 7 are consistent with the proposed structure (Figure 4).

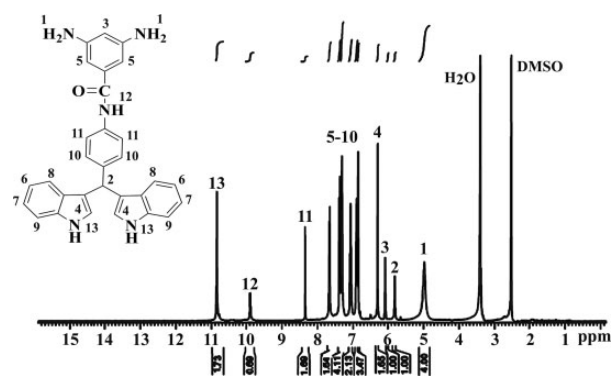


Figure 3. ^1H NMR spectrum of diamine 7 in $\text{DMSO}-d_6$ solution. ^1H NMR: Proton nuclear magnetic resonance; $\text{DMSO}-d_6$: dimethyl sulfoxide- d_6 .

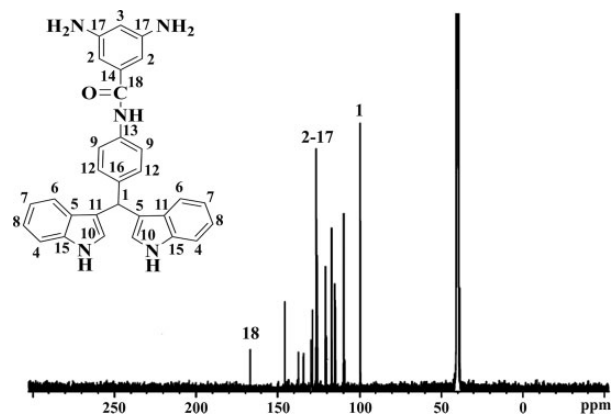


Figure 4. ^{13}C NMR spectrum of diamine 7 in $\text{DMSO}-d_6$ solution. ^{13}C NMR: Carbon-13 nuclear magnetic resonance; $\text{DMSO}-d_6$: dimethyl sulfoxide- d_6 .

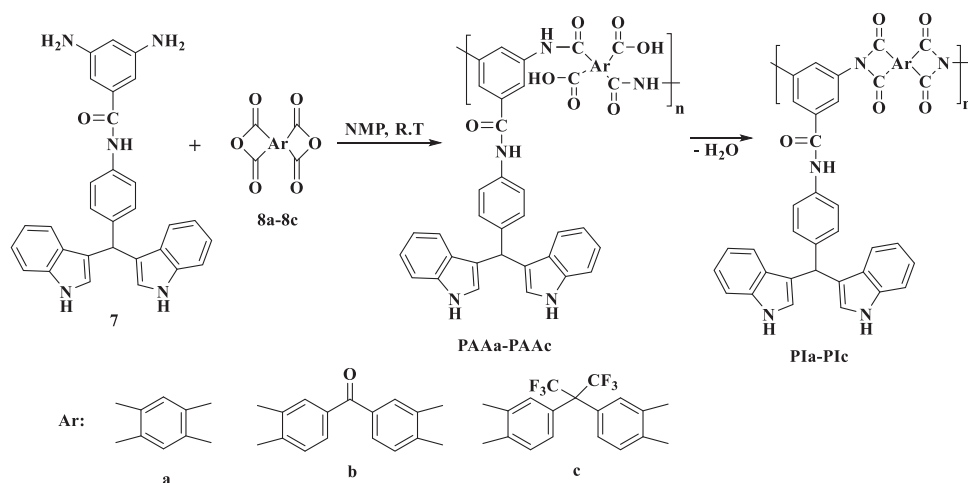


Figure 5. Preparation of PIs. PI: polyimide.

PIs synthesis

The PIs having *N*-(4-(di(1H-indole-3-yl)methyl)phenyl) units were prepared from new diamine **7** with three aromatic dianhydrides (PMDA, BTDA, and 6FDA) by the two-step polycondensation reaction via either thermal or chemical imidization techniques, as shown in Figure 5. The PAA solution was prepared by slowly adding a solution of dianhydride to a solution of the diamine **7** in dehydrated NMP. The chemical imidization of the PAA was carried out in the presence of a mixture of acetic anhydride and pyridine as a dehydrating agent. Alternatively, the thermal imidization of the PAA was occurred via heating the PAA films to the temperature 280°C under vacuum to produce PI films. The results of the polymerization reactions are reported in Table 1. Inherent viscosity values of PIs were in the range of 0.31–0.72 dL g⁻¹ showing a moderate molecular weight. These polymers generally displayed brown color due to charge transfer between the diamine donor moieties and dianhydride acceptor groups (Table 1).

Polymer characterization

The structure of the PIs was confirmed by FTIR, ¹H NMR spectroscopy, and elemental analysis. The characteristic absorption bands at 1778 and 1725 cm⁻¹ are attributed to the asymmetric and symmetric stretching of imide carbonyl groups, respectively, and an absorption band at 1367 cm⁻¹ because of C–N stretching which confirmed the formation of imide units. The results of elemental analysis of PIs are in good agreement with the theoretical content. The FTIR, ¹H NMR spectroscopy, and elemental analysis suggest the successful preparation of the PIs.

Wide-angle X-ray diffraction (XRD) is used to determine the crystalline structure of polymers. The representative X-ray powder diffraction pattern of PI-b-I is shown in Figure 6. All of the prepared polymers show similar X-ray

Table 1. Synthesis and some physical properties of PIs.

Dianhydride	Polymer	Method ^a	Yield (%)	η_{inh} (dL g ⁻¹) ^b	Color
A	PI-a-I	I	84	0.31	Brown
B	PI-b-I	I	75	0.48	Off-white
C	PI-c-I	I	79	0.35	Off-white
A	PI-a-II	II	81	0.42	Brown
B	PI-b-II	II	82	0.72	Brown
C	PI-c-II	II	78	0.38	Brown

PI: polyimide; DMF: *N,N*-dimethylformamide.

^aMethod I: chemical imidization; method II: thermal imidization.

^bMeasured at a concentration of 0.5 g dL⁻¹ in DMF at 25°C.

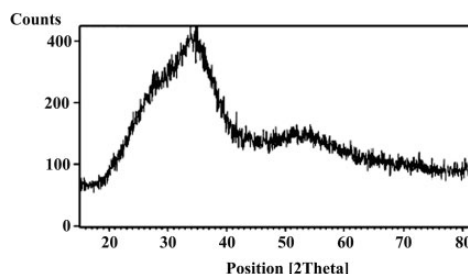


Figure 6. XRD pattern of PI-b-I. XRD: X-ray diffraction.

powder diffraction pattern. The diffraction patterns demonstrate that all the PIs are amorphous, primarily owing to the bulky *N*-(4-(di(1H-indole-3-yl)methyl)phenyl) pendant moieties. Additionally, the amorphous nature of these polymers is also reflected in their good solubility.

The mechanical properties of the PI films are summarized in Table 2. The PI films had a tensile strength of 83–107 MPa, an elongation at break range of 7–10%, and a tensile modulus range of 2.2–2.3 GPa. These polymers have a dielectric constant of 3.21–3.34. The PI films show good tensile strength, indicating that they are strong materials.

Table 2. Solubility properties of PIs.

Polymer	Solubility in various solvents ^a								
	NMP	DMAc	DMF	DMSO	THF	CHCl ₃	CH ₂ Cl ₂	Acetone	Methanol
PI-a-I	++	++	++	++	—	—	—	—	—
PI-b-I	++	++	++	++	—	—	—	—	—
PI-c-I	++	++	++	++	—	—	—	—	—
PI-a-II	±	++	±	++	—	—	—	—	—
PI-b-II	++	++	++	++	—	—	—	—	—
PI-c-II	++	++	++	++	—	—	—	—	—

PI: polyimide; DMAc: *N,N*-dimethylacetamide; DMF: *N,N*-dimethylformamide; DMSO: dimethyl sulfoxide; THF: tetrahydrofuran; ++: soluble at room temperature; +: soluble on heating; ±, partially soluble; —: insoluble even on heating.

^aQuantitative solubility was determined using 5 mg of the polymer in 0.5 mL of solvent.

Table 3. Mechanical and dielectric properties of PIs.

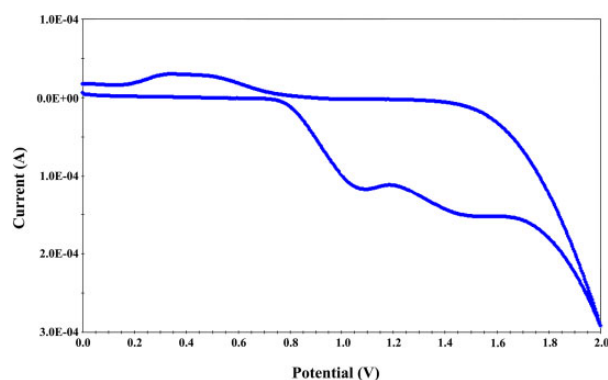
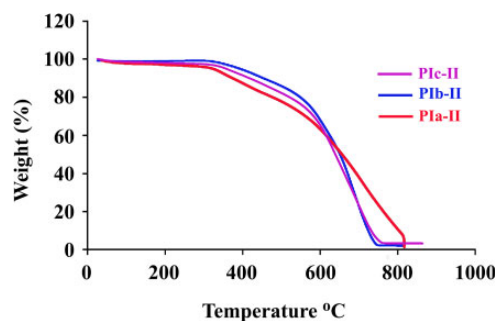
Polymer	Tensile strength (MPa)	Elongation at break (%)	Tensile modulus (GPa)	Dielectric constant (dry, 1 kHz)
PI-a-II	83	8	2.3	3.21
PI-b-II	107	6	2.2	3.34
PI-b-II	94	10	2.2	3.28

PI: polyimide.

The solubility of PIs was tested quantitatively in various solvents. All the PIs were soluble in the test solvents such as NMP, DMAc, DMF, and DMSO and were insoluble in solvents including chloroform, methylene chloride, acetone, ethanol, methanol, and water. The solubility of the PIs in several organic solvents is presented in Table 3. The good solubility should be an outcome from increased flexibility or free volume caused via the introduction of bulky pendent *N*-(4-(di(1*H*-indole-3-yl)methyl)phenyl) groups along the polymer backbone. The good solubility makes these PIs potential candidates for practical applications in spin- or dip-coating processes.

The ultraviolet–visible (UV-Vis) and photoluminescence spectra of the prepared PIs were recorded in DMF solution. The concentrations of the PIs for the UV-Vis absorption test were about 6×10^{-5} mol L⁻¹. It is apparent that the wavelength of maximum absorption is related to the $\pi \rightarrow \pi^*$ transition resulting from the conjugation between the aromatic rings and nitrogen atoms in the abovementioned polymers. All of these compounds show almost similar UV-Vis spectra pattern. These polymers revealed maximum absorption around 323 nm in DMF solution. When the PIs were excited at maximum absorption wavelength, the emission wavelengths were observed at 378 and 406 nm, respectively. All of these polymers display virtually alike fluorescence spectra pattern.

Charge transport in organic materials is believed to be governed by the hopping process involving redox reaction of charge transport molecules. CV is a preliminary

**Figure 7.** Cyclic voltammogram of PI-b-I in acetonitrile with 0.1 M Bu₄NPF₆. PI: polyimide.**Figure 8.** TGA thermograms of PIs. TGA: thermogravimetric analysis; PI: polyimide.

characterization method to determine the redox properties of polymeric materials. Figure 7 shows the representative cyclic voltammogram of the PI-a-I in acetonitrile with 0.1 M Bu₄NPF₆. One pair of redox waves was observed in these polymers. As shown in Figure 7, PI-a-I showed an oxidation wave of which a peak top is at 1.07 V (versus Ag/AgCl).

The thermal properties of PIs were calculated by TGA and DSC at a heating rate of 10°C min⁻¹, under a nitrogen atmosphere. These studies exhibit that the polymers are thermally stable up to 300°C (Figure 8). The

Table 4. Thermal properties of PIs.

Polymer	Decomposition temperature (°C)		Char yield ^c (%)	<i>T_g</i> (°C) ^d
	<i>T₅</i> ^a	<i>T₁₀</i> ^b		
PI-a-II	325	372	11	223
PI-b-II	385	451	3	264
PI-c-II	355	415	4	258

PI: polyimide; TGA: thermogravimetric analysis; *T_g*: glass transition temperature.

^aTemperature at which 5% weight loss was recorded by TGA at a heating rate of 10 °C min⁻¹ under a nitrogen atmosphere.

^bTemperature at which 10% weight loss was recorded by TGA at a heating rate of 10 °C min⁻¹ under a nitrogen atmosphere.

^cPercentage weight of material left undecomposed after TGA analysis at maximum temperature 800 °C under a nitrogen atmosphere.

^d*T_g* recorded at a heating rate of 20 °C min⁻¹ under a nitrogen atmosphere.

thermoanalysis data of these polymers are summarized in Table 4. The 10% weight loss temperatures of the aromatic PIs were recorded in 372°C, 451°C, and 415°C for PI-a-II, PI-b-II, and PI-c-II, respectively. The amount of residue (char yield) of these polymers was more than 3% at 800°C.

Conclusions

A novel aromatic diamine, 3,5-diamino-*N*-(4-(di(1H-indole-3-yl)methyl)phenyl)benzamide, was successfully prepared in high purity and good yield and applied for the preparation of high molecular-weight PIs with three aromatic tetracarboxylic dianhydrides through the two-step thermal and chemical imidization. The resulting polymers were soluble in polar aprotic solvents and displayed good thermal stability. The XRD analysis reveals the amorphous nature of PIs. The PIs could afford tough and flexible films with good mechanical properties.

Acknowledgement

The authors are grateful to the Yasouj University for financial assistance.


Declaration of conflicting interests

The author(s) declared no potential conflicts of interest with respect to the research, authorship, and/or publication of this article.

Funding

The author(s) disclosed receipt no financial support for the research, authorship, and/or publication of this article: This work was supported by Yasouj University.

ORCID iD

Zahra Rafiee  <https://orcid.org/0000-0002-4296-8760>

References

1. Dadashpour S and Emami S. Indole in the target-based design of anticancer agents: a versatile scaffold with diverse mechanisms. *Eur J Med Chem* 2018; **150**: 9–29.
2. Chadha N and Silakari O. Indoles as therapeutics of interest in medicinal chemistry: bird's eye view. *Eur J Med Chem* 2017; **134**: 159–184.
3. Chojnacki JE, Liu K, Yan X, et al. Discovery of 5-(4-hydroxyphenyl)-3-oxo-pentanoic acid [2-(5-methoxy-1H-indol-3-yl)-ethyl]-amide as a neuroprotectant for Alzheimer's disease by hybridization of curcumin and melatonin. *ACS Chem Neurosci* 2014; **5**: 690–699.
4. Gazvoda M, Krivec M, Casar Z, et al. En route to 2-(Cyclobuten-1-yl)-3-(trifluoromethyl)-1H-indole. *J Org Chem* 2018; **83**: 2486–2493.
5. Tunbridge GA, Orama J and Caggiano L. Design, synthesis and antiproliferative activity of indole analogues of indanocine. *Med Chem Commun* 2013; **4**: 1452–1456.
6. Guan Q, Han C, Zuo D, et al. Synthesis and evaluation of benzimidazole carbamates bearing indole moieties for anti-proliferative and antitubulin activities. *Eur J Med Chem* 2014; **87**: 306–315.
7. Kondreddi RR, Jiricek J, Rao SP, et al. Design, synthesis, and biological evaluation of indole-2-carboxamides: a promising class of antituberculosis agents. *J Med Chem* 2013; **56**: 8849–8859.
8. Telep El-Sayed M, Suzen S, Altanlar N, et al. Discovery of bisindolyl-substituted cycloalkane-anellated indoles as novel class of antibacterial agents against *S. aureus* and MRSA. *Bioorg Med Chem Lett* 2016; **26**: 218–221.
9. Choi Y, Abdelmegeed MA and Song BJ. Preventive effects of indole-3-carbinol against alcohol-induced liver injury in mice via antioxidant, anti-inflammatory, and anti-apoptotic mechanisms: Role of gut-liver-adipose tissue axis. *J Nutr Biochem* 2018; **55**: 12–25.
10. Jeong I, Kim J, Kim J, et al. 6-(2-Thienyl)-4H-thieno[3,2-b]indole based conjugated polymers with low bandgaps for organic solar cells. *Synth Met* 2016; **213**: 25–33.
11. Kim J, Park SY, Han G, et al. Conjugated polymers containing 6-(2-thienyl)-4H-thieno[3,2-b]indole (TTI) and iso-indigo for organic photovoltaics. *Polymer* 2016; **95**: 36–44.
12. Song YL, Wu F, Zhang CC, et al. Ionic liquid catalyzed synthesis of 2-(indole-3-yl)-thiochroman-4-ones and their novel antifungal activities. *Bioorg Med Chem Lett* 2015; **25**: 259–261.
13. Wei W, Yang L and Chang G. Heat-resistant and photoluminescent indole-based poly(ether sulfone)s. *High Perform Polym* 2017; **30**: 475–479.
14. Caste C, Castelvetro V, Ciardelli F, et al. Photoconductive films of poly-N-vinylindole-based blends for high-voltage photorefractive electrooptic cells. *Synth Met* 2003; **138**: 341–345.

15. Angelone R, Caste C, Castelvetro V, et al. Synthesis and electrooptical characterization of polysiloxanes containing indolyl groups acting as photoconductive substrates for photorefractive materials. *e-Polymers* 2004; **075**: 1–15.
16. Sroog CE. Polyimides. *Prog Polym Sci* 1991; **16**: 561–694.
17. Li J, Zhang G, Jing Z, et al. Synthesis and characterization of porous polyimide films containing benzimidazole moieties. *High Perform Polym* 2017; **29**: 869–876.
18. Ree M. High performance polyimides for applications in microelectronics and flat panel displays. *Macromol Res* 2006; **14**: 1–33.
19. Tsai CL, Yen HJ and Liou GS. Highly transparent polyimide hybrids for optoelectronic applications. *React Funct Polym* 2016; **108**: 2–30.
20. Vaganova TA, Plekhanov AI, Simanchuk AE, et al. Synthesis and characterization of novel polyhalogenaromatic polyimide material for electro-optic applications. *J Fluorine Chem* 2017; **195**: 70–78.
21. Liu Z, Yu F, Zhang Q, et al. Preparation and characterization of a novel polyimide liquid crystal vertical alignment layer. *Eur Polym J* 2008; **44**(8): 2718–2727.
22. Danev G, Assa J, Jivkov I, et al. Polyimide-matrix-based composite materials. *J Mater Sci* 2003; **14**(10): 825–827.
23. Wiegand JR, Smith ZP, Liu Q, et al. Synthesis and characterization of triptycene-based polyimides with tunable high fractional free volume for gas separation membranes. *J Mater Chem A* 2014; **2**: 13309–13320.
24. Kadiyala AK, Sharma M and Bijwe J. Exploration of thermoplastic polyimide as high temperature adhesive and understanding the interfacial chemistry using XPS, ToF-SIMS and Raman spectroscopy. *Mater Des* 2016; **109**: 622–633.
25. Zhang C, Li P and Cao B. Effects of the side groups of the spirobichroman-based diamines on the chain packing and gas separation properties of the polyimides. *J Memb Sci* 2017; **530**: 176–184.
26. Liu J, Wang K, Lin L, et al. Synthesis and property of fluorinated polyimides with double bond end groups for UV-cured coating. *Prog Org Coat* 2016; **99**: 103–109.
27. Charlier Y, Hedrick JL and Russell TP. Polyimide foams prepared from homopolymer/copolymer mixtures. *Polymer* 1995; **36**: 4529–4534.
28. Rafiee Z and Rasekh M. Preparation and characterization of polyimides containing triaryl imidazole side groups. *Polym Adv Technol* 2017; **28**(4): 533–540.
29. Zin N, McIntosh K, Bakhshi S, et al. Polyimide for silicon solar cells with double-sided textured pyramids. *Sol Energy Mater Sol* 2018; **183**: 200–204.
30. Ma X, Abdulhamid M, Miao X, et al. Facile synthesis of a hydroxyl-functionalized tröger's base diamine: a new building block for high-performance polyimide gas separation membranes. *Macromolecules* 2017; **50**(24): 9569–9576.
31. Song G, Wang L, Liu D, et al. Gas transport properties of polyimide membranes based on triphenylamine unit. *High Perform Polym* 2016; **30**: 100–108.
32. Rafiee Z and Golriz L. Synthesis and properties of thermally stable polyimides bearing pendent fluorene moieties. *Polym Adv Technol* 2014; **25**: 1523–1529.
33. Liaw DJ, Wang KL, Huang YC, et al. Advanced polyimide materials: syntheses, physical properties and applications. *Prog Polym Sci* 2012; **37**: 907–974.
34. Liaw DJ, Hsu PN, Chen WH, et al. High glass transitions of new polyamides, polyimides, and poly(amide-imide)s containing a triphenylamine group: synthesis and characterization. *Macromolecules* 2002; **35**: 4669–4676.
35. Hamciuc C, Hamciuc E, Homocianu M, et al. New blue fluorescent and highly thermostable polyimide and poly(amide-imide)s containing triphenylamine units and (4-dimethylaminophenyl)-1,3,4-oxadiazole side groups. *Dyes Pigments* 2018; **148**: 249–262.
36. Ashraf AR, Akhter Z, Simon LC, et al. Polyimide derivatives of 4,4'-bis((4-aminophenoxy)methyl)-1,1'-biphenyl: synthesis, spectroscopic characterization, single crystal XRD and thermal studies. *J Mol Struct* 2018; **1169**: 46–53.
37. Mi Z, Liu Z, Yao J, et al. Transparent and soluble polyimide films from 1,4:3,6-dianhydro-D-mannitol based dianhydride and diamines containing aromatic and semiaromatic units: Preparation, characterization, thermal and mechanical properties. *Polym Degrad Stab* 2018; **151**: 80–89.
38. Terraza CA, Tagle LH, Santiago-García JL, et al. Synthesis and properties of new aromatic polyimides containing spirocyclic structures. *Polymer* 2018; **137**: 283–292.